Published in final edited form as:
Neuron. 2011 January 27; 69(2): 273–286. doi:10.1016/j.neuron.2010.12.022.

In vivo time-lapse imaging and serial section electron microscopy reveal developmental synaptic rearrangements

Jianli Li[1], **Alev Erisir**[2], and **Hollis Cline**[1]

[1]The Scripps Research Institute, La Jolla, CA 92037

[2]Department of Psychology, University of Virginia, Charlottesville, VA 22904

Abstract

Dendrites, axons and synapses are dynamic during circuit development, however changes in microcircuit connections as branches stabilize have not been directly demonstrated. By combining in vivo time-lapse imaging of Xenopus tectal neurons with electron microscope reconstructions of imaged neurons, we report for the first time the distribution and ultrastructure of synapses on individual vertebrate neurons and relate these synaptic properties to dynamics in dendritic and axonal arbor structure over hours or days of imaging. Dynamic dendrites have a high density of immature synapses whereas stable dendrites have sparser, mature synapses. Axons initiate contacts from multisynapse boutons on stable branches. Connections are refined by decreasing convergence from multiple inputs to postsynaptic dendrites and by decreasing divergence from multisynapse boutons to postsynaptic sites. Visual deprivation or NMDAR antagonists decreased synapse maturation and elimination, suggesting that coactive input activity promotes microcircuit development by concurrently regulating synapse elimination and maturation of remaining contacts.

Keywords

in vivo imaging; ultrastructure; synapse formation; synapse maturation; 3D reconstruction; Xenopus; retinotectal system; synapse elimination

Circuit formation in the CNS requires the coordinated elaboration of axonal and dendritic arbors plus the establishment of appropriate synaptic connections and elimination of inappropriate synapses. Traditionally it is thought that a developmental period of exuberant process outgrowth and excess synapse formation occur relatively early during brain development and is followed by elimination of inappropriate synapses and pruning of axon branches (Luo and O'Leary, 2005). This view is supported by the rapid increase and subsequent protracted decrease in CNS synapse density in many species (Blue and Parnavelas, 1983; Cragg, 1975; Huttenlocher and Dabholkar, 1997; Rakic et al., 1986; Warton and McCart, 1989; Zecevic et al., 1989), and suggests that process outgrowth and synaptogenesis are temporally and mechanistically distinct from synapse elimination and branch retraction. Reports of concurrent synapse formation and elimination (Campbell and

Correspondence: Hollis Cline, Dept of Cell Biology, The Scripps Research Institute, 10550 North Torrey Pines Rd, La Jolla, CA 92037, cline@scripps.edu.

Shatz, 1992; Chen and Regehr, 2000; Katz and Shatz, 1996; Shatz and Kirkwood, 1984) suggest a program of circuit development in which selective maintenance of synapses stabilizes dendritic and axonal structures, while synapse elimination presages retraction of dendritic and axonal branches (Cline and Haas, 2008; Hua and Smith, 2004; Luo and O'Leary, 2005). Concurrent synapse elimination and synapse formation would allow relatively rapid selection of optimal synaptic partners, as seen during development and learning-based refinement of sensory and motor circuits (Guic et al., 2008; Richards et al., 2010; Ruthazer et al., 2003) and acquisition of cognitive skills (Komiyama et al., 2010). Furthermore, the possibility that synapse formation, maturation and elimination are concurrent during circuit plasticity suggests that these diverse synaptic rearrangements may be regulated by similar experience-dependent mechanisms.

Time-lapse imaging of developing neurons in intact animals or brain slices demonstrated that axonal and dendritic branches are dynamic over minutes to hours and that conditions that modify synapse formation and strength correspondingly alter the elaboration and stability of dendritic and axonal arbors (Aizenman and Cline, 2007; Alsina et al., 2001; Antonini and Stryker, 1993; Cline and Haas, 2008; Lohmann et al., 2002; Ruthazer et al., 2003; Sin et al., 2002; Wu and Cline, 1998). Nevertheless the relationship between structural dynamics of developing processes and potential synaptic rearrangements during microcircuit development are relatively unknown because direct observations of both pre- and postsynaptic structures during these events remains technically very challenging, particularly in delicate developing brain tissue. We were interested in determining whether new axonal and dendritic branches are the principle sites of synaptogenesis, whether the properties of synapses on stable dendritic or axonal branches differ from those on newly added branches, and whether synapse elimination is restricted to retracting dendritic and axonal branches.

To determine the relation between neuronal branch dynamics and the formation and elimination of synapses, we developed the reagents and methods that allow *in vivo* two-photon time-lapse imaging of fluorescently-labeled neurons in the optic tectum of Xenopus laevis tadpoles to be combined with reconstruction of serially-sectioned transmission electron microscope (TEM) images of the imaged neurons (Li et al., 2010). Live imaging was used to identify dynamic branches within neurons and serial-section TEM was used to generate a 3 dimensional reconstruction of labeled neurons and their synaptic partners. We compared the data sets to determine the distribution of synaptic connectivity and a quantitative measure of synaptic properties for dynamic and stable dendritic and axonal branches.

We report that newly extended dendritic branches and filopodia emerging from extended branches are the principle sites of synaptogenesis and that a high density of immature synapses form on newly extended dendrites. Dendritic branch stabilization correlates with a transition to sparser more mature synaptic contacts. In contrast to popular models of circuit formation, the majority of immature presynaptic sites are formed from multisynapse boutons (MSBs) on stable axon branches rather than axonal filopodia. MSBs decrease their number of connected partners to form mature connections with single postsynaptic dendrites. Finally, we show that visual experience and NMDA receptor activity are required for both synapse elimination and synapse maturation. Together these data demonstrate that dendritic and axonal branches use different strategies in the construction and refinement of synaptic circuits in the CNS and that activity-regulated synapse elimination and maturation are concurrent during the development of microcircuits.

Results

Distribution of Synaptic Contacts within the Dendritic Arbor

To map the distribution of all synaptic contacts in the dendritic arbor, we transfected single neurons with a pCMV::EGFP/mHRP construct that expresses cytosolic EGFP and membrane-targeted horseradish peroxidase (mHRP). The EGFP was used for *in vivo* 2-photon imaging, light microscopic reconstruction of the neuron at different time-points and identification of dynamic and stable dendritic and axonal branches by comparison of reconstructions from different time points. The mHRP permits identification of the imaged neuron and its pre-and post-synaptic targets using EM without obscuring the intracellular ultrastructure necessary to identify and quantify synaptic features (Figure 1A–D). Expression of this construct does not appear to affect growth rate or structural dynamics of neurons in vivo (Li et al., 2010).

To compare the configuration and ultrastructure of synapses on dynamic and stable dendritic and axonal branches within the same neurons, cells were transfected with EGFP/mHRP and imaged either at 24h intervals over 3 days (days 1, 2, and 3) or at 0h, 4h and 8h. Here we report the results of reconstructions from two intrinsic neurons that extend local axons within the optic tectum. The first neuron had been imaged with *in vivo* time-lapse 2-photon microscopy once a day over 3 days. We collected a complete series of 6038 electron micrographs from 808 serial 70nm sections, from which we generated a 3D EM reconstruction of the entire neuron including the local axon. We partially reconstructed a second neuron that had been imaged at 0h, 4h and 8h based on 1644 electron micrographs from 305 serial 70nm sections.

We first analyzed the daily time-lapse images to identify the dynamics of each dendritic and axonal branch (Fig. 1A–C). We define a branch as extending from the branch tip to the first branch point (Ruthazer et al., 2004). The neuron showed a net increase in arbor branch length over the 3-day period, comparable to growth rates reported previously (Wu and Cline, 1998). Dendritic and axonal branches showed branch dynamics. After serial EM sectioning and 3D reconstruction (supplementary movie 1), we mapped all synaptic contacts on the reconstructed dendrites of the neuron (Fig. E–F, supplementary movie 2). Synapses were identified as described (Li et al., 2010). Previous analysis of a 10μm×10μm×7μm block of serially sectioned tectal neuropil showed that presynaptic sites lacking postsynaptic profiles (Shepherd and Harris, 1998) are rarely seen in this material (Li et al., 2010).

Synapses were located in the dendritic, somatic, and axonal compartments of tectal cells, however synaptic contacts were not evenly distributed along dendritic (Fig. 1E and Fig. 2C–F) or axonal branches (see also Fig. 6). Although some synapses were located on the cell body and dendrites, synapses were relatively sparse on the primary dendrite which passes through the cell body layer of the tectum. Once the dendritic arbor branched within the tectal neuropil, synapses became more abundant. The vast majority (93%) of terminal dendritic branches received synaptic contacts, however the density of synapses varied between different dendritic branches of the same neuron (Fig. 2).

Synapse Dynamics and Branch Stability

A goal of this study was to determine the configuration of synapses on new and stable dendritic branches. One hypothesis is that new dendritic branches form few immature synapses and that synapses on stable branches are more mature and with higher density. We find that the average synapse density throughout the dendritic arbor was 0.43 synapses/μm (total of 129 synapses on 299.8μm reconstructed dendrites). As described in experimental procedures, branches can be subdivided into different categories based on their change in length at different imaging sessions. To determine whether the variation of synapse density

on different dendritic branches correlated with the dynamic behaviors of the dendrites, we compared the density of synapses on stable, extended, and retracted dendritic branches. Examples of dynamic branches from the 2 photon images are shown in Fig 2A and B. Segments of extended, stable and retracted branches and the distributions of synapses generated from the EM reconstructions are shown in Fig 2C, D, E. The types of branch dynamics observed over the time-course of the 3 images are schematized in Fig 2F. Synapse density on branches that extended between day 2 and 3 was significantly higher (0.74 ± 0.11 synapses/μm for 75.60μm in 16 branches) than branches that were stable between day 2 and 3 (0.46 ± 0.11 synapses/μm for 207.77μm in 12 branches, $p < 0.05$, Fig. 2F.). Branches that extended between day 1 and 2 had significantly higher synapse density than branches which were stable over that time interval (0.76 ± 0.09 vs 0.42 ± 0.08 synapses/μm, n=19 and 9 branches, $p < 0.05$, Fig. 2F), even though these branches may have had different dynamics between day 2 and 3. In addition, among branches which were stable between day 2 and 3, those which extended in the first two days had significantly higher synapse density than those which were stable over 3 days (0.57 ± 0.07 vs 0.27 ± 0.07 synapses/μm, n=5 and 5, $p <0.05$, Fig. 2F). Note that branches that were stable over the entire imaging session had lower synapse density than branches that showed any extension during the imaging session. In addition, two branches that retracted between day 2 and 3 had lower synapse density (0.13 ± 0.13 synapses/μm for 16.39μm in 2 branches) than other branches. This analysis shows that the density of synaptic contacts differs significantly between different branches within the same dendritic arbor. Surprisingly, the data show that dynamic, extending branches have significantly higher synapse density and that synapses are eliminated from stable branches, suggesting that there may be a competitive mechanism underlying the synapse elimination.

Tectal neurons do not have spines, but their dendrites and axons extend small protrusions, ranging in length from 400nm to 1.5μm in the EM material, which were often not detected in 2 photon images. These processes were classified as filopodia, based on their lack of microtubules. Dendritic filopodia were present at a higher density on newly extended dendritic branches (0.4 filopodia/μm, n=12) compared to stable dendritic branches (0.15 filopodia/μm, n=16, $p<0.01$). Furthermore, 60% of filopodia on extended dendrites had synapses compared to 22% of filopodia on stable dendrites (Suppl.Table 1 and Fig. 6J). Synaptic contacts on filopodia contribute 38% (18/47) and 9% (7/78) of the total synapses on extending and stable branches. Therefore, the increased synaptic density on extending dendrites is partially contributed by the synapses on dendritic filopodia. These data suggest that filopodia on extending dendrites may probe the environment for potential synaptic partners, as suggested for developing hippocampus (Fiala et al., 1998).

Decreased Divergence with Synapse Maturation

The preferential elimination of synapses from extended dendritic branches as branches stabilize suggested that the axon boutons contacting stable and extended dendritic branches may differ in their ultrastructural features. We determined the number of postsynaptic partners of individual presynaptic axonal boutons in the optic tectum of tadpoles (stage 47) and adult frog (Fig 3). The number of synaptic contacts made by individual boutons decreased significantly from 2.09 ± 0.14 (n=34) postsynaptic partners/bouton at stage 47 to 1.19 ± 0.11 (n=21) postsynaptic partners/bouton in adults ($p<0.001$, Fig. 3H). These data indicate that most axonal boutons form synapses with multiple dendrites in the dynamic developing circuit, but eliminate synapses to form one to one connections with dendrites in the relatively stable circuit in the adult brain.

We compared the axon boutons that were presynaptic to stable and extended dendritic branches in the imaged neuron to test whether a decrease in divergence through elimination of contacts from MSBs occurred as branches stabilize (Fig 3A–F). We analyzed all

postsynaptic partners (labeled and unlabeled, as shown in Fig. 3E–F) of axonal boutons that contact mHRP-labeled dendritic processes, and found that presynaptic boutons contacting stable dendritic branches had fewer postsynaptic partners than those contacting extended branches (stable: 1.38 ± 0.06, extended: 2.19 ± 0.12 postsynaptic profiles/presynaptic bouton, n=78 and 47 respectively, $p<0.001$, Fig. 3I). Furthermore, 79% of synapses on extending dendrites contacted MSBs whereas 38% of synapses on stable dendrites contacted MSBs.

Our previous studies showed that mechanisms that increased synaptic strength and maturation also stabilize dendritic branches (Haas et al., 2006), suggesting that synapses on stable branches may be more mature than those on dynamic branches. We previously reported that the proportion of the presynaptic terminal area that is occupied by clustered synaptic vesicles increased during development when synapses mature, and termed this metric the maturation index (Li and Cline, 2010). Here, we mapped the maturation index of synapses on stable, extended and retracted branches (Fig. 4A–C). We found that synapses on stable dendrites had a higher maturation index compared to those on extended dendrites (stable: 45.2 ± 1.7, n=78; extended: 35.5 ± 2.5, n=47, $p<0.001$, Fig. 4D). We also found that synapses on retracted dendrites had a low maturation index (17.7 ± 10.2, n=4 synapses), suggesting that disassembly of synaptic components occurs prior to branch retraction, consistent with our previous in vivo imaging studies (Ruthazer et al., 2006) and studies in the neuromuscular junction (Colman et al., 1997). This analysis demonstrates that synapses on stable dendrites were significantly more mature than those on extended or retracted dendrites.

Data presented above showed that synapses on extended branches tended to be clustered within 1μm of each other. Analysis of synapse maturation relative to synapse distribution on extended branches showed that synapses that were clustered within 1μm of each other were less mature, with an average maturation index of 28.9 ± 2.9 (n=33), while synapses spaced further apart than 1μm were more mature, with an average maturation index of 42.6 ± 5.0 (n=12, $p<0.05$, Fig. 4E). By contrast, synapses on stable branches were relatively mature and their maturation indices were independent of the distance between synapses (maturation index of synapses within 1μm and larger than 1μm: 45.6 ± 2.3 vs 44.7 ± 2.8, n=47 and 28, respectively). This analysis indicates that extending branches tend to have clustered immature synapses, whereas synapses on stable branches are more mature and more sparsely spaced.

The MSBs that contact mHRP-positive dendrites also contact unlabeled dendrites (Fig. 3E–F). We noticed that there is considerable heterogeneity in the maturation indices of synaptic contacts within MSBs. We compared the maturation index of pairs of synapses within the same MSB contacting mHRP-positive imaged dendrites and mHRP-negative dendrites whose dynamic history is unknown. For boutons that contact stable mHRP-labeled dendrites, the maturation indices of the synapses contacting both the mHRP-labeled and unlabeled are relatively correlated ($R^2=0.64$, Fig. 4F). The boutons that contact dynamic mHRP-labeled dendrites form synapses with more heterogeneous maturation indices, which are less correlated ($R^2=0.25$, Fig. 4F). This analysis indicates the afferents establish divergent contacts with multiple postsynaptic neurons within a limited space by using MSB structures and that divergence from individual boutons to multiple postsynaptic partners decreases such that individual MSBs lose some synaptic contacts as others remain and become mature.

Rapid Rate of Synaptic Refinement and Branch Stabilization

Retinotectal synaptogenesis visualized by in vivo 2 photon time-lapse imaging of fluorescent protein-tagged synaptic vesicle proteins indicates that presynaptic sites assemble

over a time-course of hours (Alsina et al., 2001; Meyer and Smith, 2006; Ruthazer et al., 2006). To examine the configuration of nascent synapses formed on recently extending dendrites, we collected images of tectal neurons at 0h, 4h and 8h, a protocol we previously demonstrated captures branch dynamics (Sin et al., 2002). We created a partial 3D EM reconstruction of a dendritic arbor imaged with this rapid protocol and mapped the locations of synapses on stable and extending dendrites (Fig. 5A–M). Synapse density on dendrites extended within the previous 4h (0.67 ± 0.12 synapses/μm for 42.6μm in 6 branches) was significantly higher than on branches that were stable over the 4h imaging period (0.42 ± 0.07 synapses/μm for 73.9μm in 5 branches, $p<0.05$, Fig. 5N). In addition, we often observed that axonal boutons contacting extending dendrites, which had at most a 4h lifetime, contained dense core vesicles (Fig. 5M), consistent with the idea that they are involved in synaptogenesis (Li and Cline, 2010). As observed in the neuron imaged at daily intervals (Fig 2A), extending dendrites formed synapses with MSBs. Axon boutons contacting extending dendrites had more postsynaptic partners than boutons contacting stable dendrites (extended: 1.95±0.18, n=23; stable: 1.35±0.09, n=29; $p<0.05$, Fig. 5O). Furthermore, when we determined the average maturation index of synapses in each MSB, we found that MSBs contacting extending branches had lower average maturation indices than MSBs contacting stable dendrites (17.8±2.4 vs 41.1±2.2, n=23 and 29, $p<0.05$, Fig. 5P). As described above, the MSBs contacting the mHRP-labeled dendrites from the imaged neuron also contact neighboring unlabeled dendrites. We find significant variation in the maturation index of synapses within the same bouton that contacts extending mHRP-positive and mHRP-negative dendrites ($R^2=0.08$ Fig. 5Q), which is greater than the variation seen in synapses samples from the neuron imaged at daily intervals, where $R^2=0.25$. These data indicate that synaptic rearrangements associated with branch extension and stabilization occur at least over a time-course of hours.

Synapse Maturation and Axon Branch Dynamics

The analysis of synaptic contacts revealed a conversion from clustered immature synaptic contacts on extending dendrites to fewer mature contacts onto stable dendrites. This is accompanied by decreased divergence, measured as the number of postsynaptic profiles contacted by individual presynaptic boutons. The results suggest that presynaptic boutons undergo structural reorganization, corresponding to the dynamics of axon branches. We hypothesized that a reduction in the dynamic behaviors of axon branches would reflect a conversion from immature to mature synaptic contacts. We therefore conducted an analysis of synaptic circuit formation from the point of view of the axon. The labeled neuron imaged at daily intervals had an elaborate local axon arbor that exhibited dynamic branch extension, stabilization, and retraction (Fig. 6A). We identified a total of 170 axodendritic and axosomatic synaptic contacts from 102 boutons made by 374.3μm of reconstructed axon branches for an average synapse density of 0.45 synapses/μm of axon branch length.

We examined the ultrastructural features of the presynaptic boutons with respect to the dynamics of the axon branches based on the *in vivo* two-photon images (Fig. 6A–F). We analyzed 203.40μm from 14 stable branches, 107.81μm from 9 extended branches, and 63.09μm from 10 retracted branches. Unlike dendrites, the synapse density of stable axon branches was significantly higher than that of extended and retracted branches (stable: 0.62 ± 0.03 synapses/μm; extended: 0.27 ± 0.04 synapses/μm, $p<0.001$; retracted: 0.21 ± 0.05 synapses/μm, $p<0.001$, post hoc Mann-Whitney test after Kruskal-Wallis test, Fig. 6G). The synapses formed by stable axon branches were significantly more mature than synapses formed by extended and retracted axon branches (maturation index; stable: 41.91 ± 1.48, n=130; extended: 26.02 ± 2.67, n=26, $p<0.05$; retracted: 30.65 ± 2.58, n=14, $p<0.05$, post hoc Kruskal-Wallis test, Fig. 6H). When we analyzed the divergence of individual presynaptic boutons, we found that each axon bouton contacted between one to four

partners. In contrast to dendrites, presynaptic boutons from stable axon branches form connections with more postsynaptic partners than boutons from extended or retracted axon branches (stable: 1.83 ± 0.09 connections/bouton, n=71; extended: 1.37 ± 0.11 connections/bouton, n=19, $p<0.005$; retracted: 1.08 ± 0.18 connections/bouton, n=9, $p<0.01$, post hoc Kruskal-Wallis test, Fig. 6I). Similar to dendritic filopodia, axonal filopodia were found at a higher density on extended axon branches (0.24 filopodia/μm) compared to stable axon branches (0.12 filopodia/μm, $p<0.05$), but in contrast to dendritic filopodia, only 12% of axonal filopodia (stable or dynamic) form synapses (Fig. 6J). Our results indicate that the majority of new synaptic connections are generated from stable axon branches.

In the analysis reported above, we found that presynaptic boutons contacting stable dendritic branches had more mature synapses and contacted fewer postsynaptic partners than axonal boutons contacting extending dendrites. This suggests that there may be two groups of axon boutons on stable axon branches. Indeed, the average maturation index of connections from individual boutons on stable axon branches was inversely correlated with the number of connected postsynaptic partners. The average maturation index of boutons with 1 or 2 partners was greater than boutons with 3 or 4 partners (1–2 partners: 43.6 ± 1.9, n= 60; 3–4 partners: 33.8 ± 3.7, n=11, $p<0.05$). Furthermore, the maturation indices of the two synapses from axon boutons with only 2 postsynaptic profiles (PSPs) are more highly correlated ($R^2=0.43$) than the indices of synapses in boutons contacting 3 or 4 PSPs ($R^2=0.04$; Fig 6K). This analysis suggests that boutons with fewer postsynaptic partners and more mature synapses are more likely to be presynaptic to stable dendritic branches. The data also suggest that a signal from boutons coordinates the maturation of divergent synapses. Alternately, in a situation analogous to the process of synapse elimination at the neuromuscular junction, when two postsynaptic profiles remain in contact with a single bouton, both appear equivalent, until one profile eventually ‘wins’ while the other is eliminated.

Activity-dependent mHRP Labeling of Synaptic Vesicles

Presynaptic terminals of mHRP-labeled axons contain mHRP-labeled synaptic vesicles, which were likely labeled by endocytosis of the mHRP-labeled plasma membrane. The labeled vesicles are sparsely distributed in the presynaptic terminal and preferentially located at the periphery of the active zone (Fig. 6C–F and Fig. 7A–C), consistent with previously reported sites of vesicle endocytosis (Rizzoli and Betz, 2004). Exposure to 1μM TTX for 2h and 6h decreased the density of labeled vesicles to 50% and 11% of controls, respectively (Fig. 7D), which suggests that the mHRP labeling reports a window of prior synaptic activity on the order of 6h. This window likely reflects the rate of acidification of synaptic vesicles and the pH-sensitivity of HRP, because the optimal pH for HRP enzyme activity is 6.0–6.5 (Schomberg et al., 1993) while the pH in synaptic vesicles is ~ 5.2 (Miesenbock et al., 1998). Axon boutons with more mature synapses tend to contain a higher density of mHRP-labeled vesicles compared to boutons with immature contacts (Fig. 7E). Boutons from stable axon branches have a significantly higher density of mHRP-labeled vesicles than boutons from extended or retracted axon branches (48.05 ± 4.19 vs 25.27 ± 0.11 vesicles/ μm^2, $p<0.001$ or 27.92 ± 3.09 vesicles/ μm^2, $p<0.05$; n=62, 17, and 9, post hoc Kruskal-Wallis test, Fig. 7F). This result demonstrates that the density of mHRP-labeled vesicles reports presynaptic activity and that boutons from stable axon branches are more active than those from extended and retracted axon branches. In addition, the density of labeled synaptic vesicles in boutons along individual axonal branches fluctuated (Fig. 7G), suggesting that release behavior of boutons within the same branch is heterogeneous.

Activity-dependent Synapse Maturation and Elimination

Our data indicate that activity-dependent maturation (or strength) of synaptic contacts but not number of synapses per se stabilizes dendritic branches. To test this hypothesis directly, we analyzed two in vivo manipulations of visual input to the optic tectum: visual deprivation to decrease visually-driven correlated input activity and MK801 to block NMDAR activity. Previous work demonstrated that NMDAR blockers prevent the stabilization of retinotectal synaptic contacts assessed by time-lapse imaging of synaptophysin-CFP puncta in retinotectal axons (Ruthazer et al., 2006) and increase branch dynamics of both tectal neurons and the presynaptic retinal axon arbors (Rajan and Cline, 1998; Rajan et al., 1999). Tadpoles were visually deprived or exposed to 10μM MK801 for three days from stage 44 to stage 47 and were fixed and processed for EM. We generated serial section EM reconstructions of 97.4μm of dendrites and their presynaptic terminals from visually-deprived tadpoles and 67.6μm of dendrites and their presynaptic terminals from MK801-treated tadpoles. Exposure to either MK801 or visual deprivation decreased synapse maturation (maturation index, control: 33.4±1.4; visual deprivation: 28.8±1.9, $p<0.05$; MK801: 23.5±2.0, $p<0.05$. n=176, 92, and 108 synapses, post hoc Kruskal-Wallis test. Fig. 8B). Moreover, animals treated with MK801 or visual deprivation had higher synapse density, indicating a decrease in synapse elimination (control: 0.63±0.12 synapses/μm; visual deprivation: 1.09±0.14 synapses/μm, $p <0.05$; MK801: 0.83±0.07 synapses/μm, $p <0.05$. n=29, 15 and 10 branches, post hoc Kruskal-Wallis test. Fig. 8A,C–D). These results indicate that correlated synaptic input activity promotes circuit formation by eliminating some synaptic inputs and strengthening others.

Discussion

The ultrastructural analysis of synapse formation and maturation, combined with our knowledge of prior *in vivo* dendritic and axonal branch dynamics lead us to propose a model in which synapse elimination plays a prominent role in CNS synaptic microcircuit assembly. Newly extended dendritic branches and the filopodia they support search for partners and preferentially make connections with MSBs from stable axonal branches. The newly extended dendrites are the synaptic targets of several presynaptic boutons, resulting in a high density of immature synaptic contacts on dynamic dendrites. In contrast to dendrites, newly added axon branches are not the principle sites of synapse formation. Most presynaptic connections are initiated from MSBs located on stable axon branches, with each individual bouton forming connections with several surrounding dendritic branches. As dendritic branches stabilize, several features of synaptic connectivity change in an activity-dependent manner: individual presynaptic boutons decrease their number of postsynaptic partners, clustered convergent synaptic inputs are eliminated from stabilized dendrites and the remaining synapses mature. The data indicate that dendrites and axons use different wiring strategies during the construction of brain circuits.

Synapse Elimination and Circuit Development

Large-scale axon retraction and synapse elimination are widely recognized to play a role in circuit development by pruning exuberant connections. This has been documented extensively in developing neuromuscular, corticospinal, and cerebellar connections, and sensory systems of mammals and non-mammalian vertebrates (Cline, 2001; Huberman, 2007; Katz and Shatz, 1996; Luo and O'Leary, 2005; Nakamura and O'Leary, 1989; Purves and Lichtman, 1980; Sanes and Lichtman, 1999; Williams and McLoon, 1991). Establishment of retinogeniculate eye-specific lamination serves as an example of this mechanism of circuit development: individual retinogeniculate axons extend branches into inappropriate laminae of the lateral geniculate nucleus (LGN), which are subsequently withdrawn (Sretavan and Shatz, 1984). Serial EM reconstructions of axon branches destined

to be retracted from inappropriate LGN laminae show that they form synapses with LGN neurons and that the transient synapses are immature, based on a low density of presynaptic vesicles (Campbell and Shatz, 1992). Functionally, this is seen as a decrease in convergent inputs to postsynaptic neurons and an increase in synaptic strength of the remaining retinogeniculate inputs (Chen and Regehr, 2000; Hooks and Chen, 2006).

Here, we demonstrate that synapse elimination also plays a prominent role in CNS microcircuit development. We identify two types of synapse elimination that contribute to the refinement of CNS circuits: a reduced divergence of contacts from MSBs and a decreased convergence of multiple inputs to individual dendrites. The consequences of these rearrangements include a greater specificity of connectivity within the visual circuit, consistent with greater spatial and temporal control of visual information processing (Ruthazer and Aizenman, 2010).

Several studies suggest that the mechanisms of synapse elimination that we observe in the developing Xenopus visual system are employed during circuit development in other species. In rodent hippocampus, dendritic filopodia and MSBs are much more prevalent in young animals than older animals (Fiala et al., 1998). Our data, together with data showing a gradual reduction in synapse density in developing CNS regions from several vertebrate species (Blue and Parnavelas, 1983; Cragg, 1975; Huttenlocher and Dabholkar, 1997; Rakic et al., 1986; Warton and McCart, 1989), suggest that decreased convergence of synapses on developing dendrites together with decreased divergence of contacts from MSBs, both of which occur by synapse elimination, are mechanisms that function widely during circuit maturation.

Several technical aspects of our experiments were essential to drawing our conclusions. One is that we were able to compare synaptic density and ultrastructural features of connections onto stable and extending dendritic branches within the same dendritic arbors. Consequently, it is clear that differences in synapse density and maturation on stable and dynamic branches do not arise from heterogeneity of the postsynaptic neurons. This analysis also allows us to conclude that mature synapses are found preferentially on stable dendritic branches. Second, we were able to compare connectivity of presynaptic boutons as they relate to the dynamics of axon branches. This demonstrated that the reduced divergence from MSBs and the decreased convergence onto stable dendrites seen in this study are not necessarily accompanied by large-scale changes in axonal or dendritic arbor structure and would not have been detected without the combined use of in vivo time-lapse imaging to distinguish stable and dynamic branches, and the spatial resolution of EM. High density clusters of immature synapses on newly extended dendrites would be difficult to distinguish from fewer more mature synapses on stable dendrites based on fluorescent light microscopy of synaptic markers. Similarly, because the distances between individual synaptic contacts within a MSB are less than 1μm, the gain or loss of contacts from MSBs occurs at a sub-optical resolution, and may have been underestimated in previous light microscope based studies (Alsina et al., 2001; Meyer and Smith, 2006; Ruthazer et al., 2006). Third, we have been able to make direct comparisons between the synaptic rearrangements that occur over a 24h time interval and a 4h interval, which indicate that synapse formation, maturation and elimination occur over a time-scale of hours during activity-dependent microcircuit development in vivo. Consequently, our experiments provide direct evidence for a previously unrecognized role for synaptic dynamics and synapse elimination in fine-scale circuit development.

Synaptic Regulation of Neuronal Branch Dynamics

The potential role of synaptic connections in regulating the elaboration of neuronal structure has been proposed by Vaughn in the synaptotrophic model of neuronal development

(Vaughn, 1989), which states that formation of synaptic connections stabilize pre- and postsynaptic neuronal branches and promote further growth of the neuronal arbor. Studies in which synaptic activity was shown to regulate neuronal arbor development provide support for the synaptotrophic hypothesis (Cline and Haas, 2008), however other studies suggested that neuronal development can occur without synaptic transmission (Verhage et al., 2000). Using fluorescent protein tagged pre- or postsynaptic markers, such as synaptophysin, VAMP, or PSD95, several studies demonstrated that the presence of synaptic contacts stabilizes axonal and dendritic branches against retraction and promotes further branch additions (Alsina et al., 2001; Hua and Smith, 2004; Meyer and Smith, 2006; Niell et al., 2004; Ruthazer et al., 2003; Ruthazer et al., 2006; Sanchez et al., 2006). Nevertheless, these studies were limited by analysis of either pre- or postsynaptic neurons and the relatively low spatial resolution of fluorescence light microscopy. Questions such as whether new axonal or dendritic branches initiate synaptic contacts, whether synaptic contacts are required to stabilize branches and whether synaptic activity affects synaptic contacts on new branches had not been directly addressed. Our results clearly demonstrate that newly extended dendritic branches not only form synapses, but surprisingly, they have a significantly higher synapse density than stable branches. Extending dendritic branches have a higher density of filopodia than stable branches and 60% of filopodia on extending dendritic branches have synapses, consistent with previous observations that dendritic filopodia are sites of synaptogenesis (Fiala et al., 1998; Nikolakopoulou et al., 2010; Toni et al., 2007), Note that the dendritic filopodia analyzed by EM in this study are too small to be observed by in vivo imaging. The increased synapse maturation on stable dendritic branches is consistent with the proposed role of synapses in stabilizing neuronal structures. Similarly in axons, the increase in synaptic maturation and decrease in divergence of contacts with stable dendrites support the synaptotrophic hypothesis. Therefore our data provide further support for the synaptotrophic hypothesis by demonstrating that activity-dependent synapse maturation correlates with dendritic branch stabilization. It is interesting to note that the extensive synapse elimination we observe was not directly predicted by the synaptotrophic hypothesis, and suggests that fewer stronger synapses are more effective at stabilizing developing axons and dendrites.

In contrast to dendrites, MSBs on stable axon branches are the principle sites of synaptogenesis and new synapses were rarely found on axon filopodia. MSBs have been observed throughout the CNS in both developing and adult tissue, however the relation between MSBs and circuit development is unclear, partly because in vivo imaging with presynaptic markers cannot resolve synaptogenesis at MSBs (Meyer and Smith, 2006; Ruthazer et al., 2006). Therefore our ability to characterize inputs onto dynamic and stable dendritic branches has allowed us to demonstrate that dynamic dendrites preferentially contact MSBs compared to stable dendrites within the same arbor. New dendritic spines in adult brain preferentially synapse with MSBs (Knott et al., 2006; Toni et al., 2007). Together the data suggest that MSBs play a specific role in microcircuit development by providing higher interconnectivity within a relatively small volume, regardless of whether such dynamics occur in the developing or adult CNS.

The Time-course of Synapse Refinements in vivo

We collected data from neurons imaged either at daily intervals over 3 days or at 4h intervals over 8h (0h, 4h and 8h) and compared synapse density and ultrastructural features of synapses from newly extended and stable branches within each neuron. Our EM data indicate that all stable and extending dendritic branches form synapses and that approximately 60% of dendritic filopodia on extended branches have synapses. The data collected at the higher temporal resolution reveal a comparable decrease in synapse density and increase in synapse maturation as seen for the neuron imaged at 24h intervals,

suggesting that synaptic rearrangements relating to branch stabilization can occur within hours. This rapid time-course of synaptic rearrangements is consistent with in vivo time-lapse imaging data showing that retinotectal presynaptic puncta assemble within 6h (Ruthazer et al., 2006), that the average lifetime of dynamic dendritic branches is less than 4h, and that decreasing glutamatergic synaptic transmission decreases dendritic branch lifetimes (Haas et al., 2006; Rajan and Cline, 1998). By contrast, although some studies suggest that synapses can form within a few hours in hippocampal slices from young or mature animals (Fischer et al., 1998; Kirov et al., 1999), other studies from cultured hippocampal slices and from adult neocortex imaged in vivo indicate that synapse formation in rodent CNS is protracted over many hours to days and that synapse formation is delayed by hours compared to spine formation (Knott et al., 2006; Nagerl et al., 2007). The rapid time-course of synaptic rearrangements we observe in *Xenopus* is likely related to developmental plasticity.

Activity-dependent Synapse Elimination

Sensory inputs regulate the refinement of central sensory projections by controlling neuronal branch dynamics and synaptic strength through mechanisms including NMDA receptor activity (Constantine-Paton et al., 1990; Lee et al., 2005; McAllister, 2007; Sorensen and Rubel, 2006; Wong and Ghosh, 2002). Comparable mechanisms likely underlie synaptic reorganization throughout the CNS. Activity-dependent synapse elimination has been documented in the Xenopus visual system (Ruthazer et al., 2003; Ruthazer et al., 2006) and in mammalian sensory projections (Hooks and Chen, 2006, 2008; Lee et al., 2005; Wang and Zhang, 2008) and cerebellum (Bosman et al., 2008). Our ultrastructural data demonstrate that decreasing correlated afferent activity by depriving animals of visual experience, or blocking the postsynaptic detection of correlated input activity with the NMDAR antagonist MK801 increased synapse density and decreased synapse maturation, consistent with the idea that decreasing correlated inputs prevented both synapse elimination and maturation. These experiments show that activity-dependent synapse elimination mediates the decrease in divergence of contacts from MSBs and the decrease in synaptic convergence onto stabilized dendritic branches. Clustered synaptic inputs likely enable extended dendritic branches and filopodia to test for correlated input activity from several potential presynaptic partners (Stepanyants et al., 2002). Similarly MSBs enable presynaptic axons to sample several postsynaptic partners. Together activity-dependent synapse elimination and maturation contribute to the experience-dependent refinement of the retinotectal projection.

In conclusion, this study combined in vivo time-lapse 2-photon imaging with serial section EM-based 3D reconstruction of two intrinsic optic tectal neurons to identify the mechanisms of synaptic refinement during circuit development. By interpreting ultrastructural features of synaptic connectivity in light of structural dynamics of axons and dendrites, we demonstrate a prominent role of synapse elimination in experience-dependent circuit refinement. In light of the considerable attention now being focused on the possibility of determining connectivity maps of CNS circuits (Bohland et al., 2009; Chou et al.; Lichtman et al., 2008; Lu et al., 2009), this study demonstrates the degree of microcircuit dynamics that can occur in the developing CNS.

Experiment Procedures

All experimental protocols were approved by the Cold Spring Harbor Laboratory Animal Care and Use Committee and complied with the guidelines established in the Public Health Service Guide for the Care and Use of Laboratory Animals.

Single cell electroporation and time-lapse imaging

Single optic tectal neurons in stage 44 Xenopus laevis tadpoles were transfected by single cell electroporation (Bestman et al., 2006) with a construct with two CMV promoters that expresses both EGFP and mHRP, called pCMV::EGFP/mHRP, as described in detail (Li et al., 2010). We collected 2-photon images once a day over 3 days (day 1, 2, and 3) or every 4 hours over 8 hours (0h, 4h, 8h) and arbor structure was analyzed as described previously (Ruthazer et al., 2004) and in more detail in Supplementary Methods.

Immunohistochemistry and 3D electron microscopy reconstruction

Tissue was processed for electron microscopy as described in detail in Supplementary Methods and in (Li et al., 2010). We used RECONSTRUCT™ software (freely available from synapses.clm.utexas,edu) (Fiala, 2005) for 3D reconstruction (Li and Cline, 2010).

Data Analysis and Statistics—Detailed descriptions of the methods used to quantify synaptic maturation and divergence of contacts from individual presynaptic boutons during CNS development have been published (Haas et al., 2006; Li and Cline, 2010) and are described in Supplementary Methods. The Mann-Whitney test was used for statistical comparisons between 2 data sets. The Kruskal-Wallis test with posthoc analysis was used for comparison between 3 groups. Data are presented as mean ± standard error of the mean (s.e.m.), and all error bars are s.e.m.. The alpha of the confidence level was set at 0.05.

Supplementary Material

Refer to Web version on PubMed Central for supplementary material.

Acknowledgments

Supported by the NIH (RO1 EY-011261, EY-011261-14S1, DP10D000458 (HTC) and RO1-EY12138 (AE)). We thank Dr. Mitya Chklovski for help aligning image stacks, Stephen Hearn of the Cold Spring Harbor Laboratory Electron Microscopy Facility, Dr. Martha Bickford for her helpful insight and members of the Cline lab for discussions.

References

Aizenman CD, Cline HT. Enhanced visual activity in vivo forms nascent synapses in the developing retinotectal projection. J Neurophysiol 2007;97:2949–2957. [PubMed: 17267761]

Alsina B, Vu T, Cohen-Cory S. Visualizing synapse formation in arborizing optic axons in vivo: dynamics and modulation by BDNF. Nat Neurosci 2001;4:1093–1101. [PubMed: 11593233]

Antonini A, Stryker MP. Rapid remodeling of axonal arbors in the visual cortex. Science 1993;260:1819–1821. [PubMed: 8511592]

Bestman JE, Ewald RC, Chiu SL, Cline HT. In vivo single-cell electroporation for transfer of DNA and macromolecules. Nat Protoc 2006;1:1267–1272. [PubMed: 17406410]

Blue ME, Parnavelas JG. The formation and maturation of synapses in the visual cortex of the rat. II. Quantitative analysis. J Neurocytol 1983;12:697–712. [PubMed: 6619907]

Bohland JW, Wu C, Barbas H, Bokil H, Bota M, Breiter HC, Cline HT, Doyle JC, Freed PJ, Greenspan RJ, et al. A proposal for a coordinated effort for the determination of brainwide neuroanatomical connectivity in model organisms at a mesoscopic scale. PLoS Comput Biol 2009;5:e1000334. [PubMed: 19325892]

Bosman LW, Takechi H, Hartmann J, Eilers J, Konnerth A. Homosynaptic long-term synaptic potentiation of the "winner" climbing fiber synapse in developing Purkinje cells. J Neurosci 2008;28:798–807. [PubMed: 18216188]

Campbell G, Shatz CJ. Synapses formed by identified retinogeniculate axons during the segregation of eye input. J Neurosci 1992;12:1847–1858. [PubMed: 1578274]

Chen C, Regehr WG. Developmental remodeling of the retinogeniculate synapse. Neuron 2000;28:955–966. [PubMed: 11163279]

Chou YH, Spletter ML, Yaksi E, Leong JC, Wilson RI, Luo L. Diversity and wiring variability of olfactory local interneurons in the Drosophila antennal lobe. Nat Neurosci 2010;13:439–449. [PubMed: 20139975]

Cline H, Haas K. The regulation of dendritic arbor development and plasticity by glutamatergic synaptic input: a review of the synaptotrophic hypothesis. J Physiol 2008;586:1509–1517. [PubMed: 18202093]

Cline HT. Dendritic arbor development and synaptogenesis. Current Opinion in Neurobiology 2001;11:118–126. [PubMed: 11179881]

Colman H, Nabekura J, Lichtman JW. Alterations in synaptic strength preceding axon withdrawal. Science 1997;275:356–361. [PubMed: 8994026]

Constantine-Paton M, Cline HT, Debski E. Patterned activity, synaptic convergence, and the NMDA receptor in developing visual pathways. Annu Rev Neurosci 1990;13:129–154. [PubMed: 2183671]

Cragg BG. The development of synapses in the visual system of the cat. J Comp Neurol 1975;160:147–166. [PubMed: 1112924]

Fiala JC. Reconstruct: a free editor for serial section microscopy. J Microsc 2005;218:52–61. [PubMed: 15817063]

Fiala JC, Feinberg M, Popov V, Harris KM. Synaptogenesis via dendritic filopodia in developing hippocampal area CA1. J Neurosci 1998;18:8900–8911. [PubMed: 9786995]

Fischer M, Kaech S, Knutti D, Matus A. Rapid actin-based plasticity in dendritic spines. Neuron 1998;20:847–854. [PubMed: 9620690]

Guic E, Carrasco X, Rodriguez E, Robles I, Merzenich MM. Plasticity in primary somatosensory cortex resulting from environmentally enriched stimulation and sensory discrimination training. Biol Res 2008;41:425–437. [PubMed: 19621123]

Haas K, Li J, Cline HT. AMPA receptors regulate experience-dependent dendritic arbor growth in vivo. Proc Natl Acad Sci U S A 2006;103:12127–12131. [PubMed: 16882725]

Hooks BM, Chen C. Distinct roles for spontaneous and visual activity in remodeling of the retinogeniculate synapse. Neuron 2006;52:281–291. [PubMed: 17046691]

Hooks BM, Chen C. Vision triggers an experience-dependent sensitive period at the retinogeniculate synapse. J Neurosci 2008;28:4807–4817. [PubMed: 18448657]

Hua JY, Smith SJ. Neural activity and the dynamics of central nervous system development. Nat Neurosci 2004;7:327–332. [PubMed: 15048120]

Huberman AD. Mechanisms of eye-specific visual circuit development. Curr Opin Neurobiol 2007;17:73–80. [PubMed: 17254766]

Huttenlocher PR, Dabholkar AS. Regional differences in synaptogenesis in human cerebral cortex. J Comp Neurol 1997;387:167–178. [PubMed: 9336221]

Katz LC, Shatz CJ. Synaptic activity and the construction of cortical circuits. Science 1996;274:1133–1138. [PubMed: 8895456]

Kirov SA, Sorra KE, Harris KM. Slices have more synapses than perfusion-fixed hippocampus from both young and mature rats. J Neurosci 1999;19:2876–2886. [PubMed: 10191305]

Knott GW, Holtmaat A, Wilbrecht L, Welker E, Svoboda K. Spine growth precedes synapse formation in the adult neocortex in vivo. Nat Neurosci 2006;9:1117–1124. [PubMed: 16892056]

Komiyama T, Sato TR, O'Connor DH, Zhang YX, Huber D, Hooks BM, Gabitto M, Svoboda K. Learning-related fine-scale specificity imaged in motor cortex circuits of behaving mice. Nature 2010;464:1182–1186. [PubMed: 20376005]

Lee LJ, Lo FS, Erzurumlu RS. NMDA receptor-dependent regulation of axonal and dendritic branching. J Neurosci 2005;25:2304–2311. [PubMed: 15745956]

Li J, Cline HT. Visual deprivation increases accumulation of dense core vesicles in developing optic tectal synapses in Xenopus laevis. J Comp Neurol 2010;518:2365–2381. [PubMed: 20437533]

Li J, Wang Y, Chiu SL, Cline HT. Membrane targeted horseradish peroxidase as a marker for correlative fluorescence and electron microscopy studies. Front Neural Circuits 2010;4:6. [PubMed: 20204144]

Lichtman JW, Livet J, Sanes JR. A technicolour approach to the connectome. Nat Rev Neurosci 2008;9:417–422. [PubMed: 18446160]

Lohmann C, Myhr KL, Wong RO. Transmitter-evoked local calcium release stabilizes developing dendrites. Nature 2002;418:177–181. [PubMed: 12110889]

Lu J, Tapia JC, White OL, Lichtman JW. The interscutularis muscle connectome. PLoS Biol 2009;7:e32. [PubMed: 19209956]

Luo L, O'Leary DD. Axon retraction and degeneration in development and disease. Annu Rev Neurosci 2005;28:127–156. [PubMed: 16022592]

McAllister AK. Dynamic aspects of CNS synapse formation. Annu Rev Neurosci 2007;30:425–450. [PubMed: 17417940]

Meyer MP, Smith SJ. Evidence from in vivo imaging that synaptogenesis guides the growth and branching of axonal arbors by two distinct mechanisms. J Neurosci 2006;26:3604–3614. [PubMed: 16571769]

Miesenbock G, De Angelis DA, Rothman JE. Visualizing secretion and synaptic transmission with pH-sensitive green fluorescent proteins. Nature 1998;94:192–195. [PubMed: 9671304]

Nagerl UV, Kostinger G, Anderson JC, Martin KA, Bonhoeffer T. Protracted synaptogenesis after activity-dependent spinogenesis in hippocampal neurons. J Neurosci 2007;27:8149–8156. [PubMed: 17652605]

Nakamura H, O'Leary DD. Inaccuracies in initial growth and arborization of chick retinotectal axons followed by course corrections and axon remodeling to develop topographic order. J Neurosci 1989;9:3776–3795. [PubMed: 2585055]

Niell CM, Meyer MP, Smith SJ. In vivo imaging of synapse formation on a growing dendritic arbor. Nat Neurosci 2004;7:254–260. [PubMed: 14758365]

Nikolakopoulou AM, Meynard MM, Marshak S, Cohen-Cory S. Synaptic maturation of the Xenopus retinotectal system: effects of brain-derived neurotrophic factor on synapse ultrastructure. J Comp Neurol 2010;518:972–989. [PubMed: 20127801]

Purves D, Lichtman JW. Elimination of synapses in the developing nervous system. Science 1980;210:153–157. [PubMed: 7414326]

Rajan I, Cline HT. Glutamate receptor activity is required for normal development of tectal cell dendrites in vivo. J Neurosci 1998;18:7836–7846. [PubMed: 9742152]

Rajan I, Witte S, Cline HT. NMDA receptor activity stabilizes presynaptic retinotectal axons and postsynaptic optic tectal cell dendrites in vivo. J Neurobiol 1999;38:357–368. [PubMed: 10022578]

Rakic P, Bourgeois JP, Eckenhoff MF, Zecevic N, Goldman-Rakic PS. Concurrent overproduction of synapses in diverse regions of the primate cerebral cortex. Science 1986;232:232–235. [PubMed: 3952506]

Richards BA, Voss OP, Akerman CJ. GABAergic circuits control stimulus-instructed receptive field development in the optic tectum. Nat Neurosci 2010;13:1098–1106. [PubMed: 20694002]

Rizzoli SO, Betz WJ. The structural organization of the readily releasable pool of synaptic vesicles. Science 2004;303:2037–2039. [PubMed: 15044806]

Ruthazer ES, Aizenman CD. Learning to see: patterned visual activity and the development of visual function. Trends Neurosci 2010;33:183–192. [PubMed: 20153060]

Ruthazer ES, Akerman CJ, Cline HT. Control of axon branch dynamics by correlated activity in vivo. Science 2003;301:66–70. [PubMed: 12843386]

Ruthazer, ES.; Haas, K.; Javaherian, A.; Jensen, K.; Sin, W-C.; Cline, HT. In vivo time-lapse imaging of neuronal development. In: Yuste, R.; Konnerth, A., editors. Imaging in Neuroscience and Development. Cold Spring Harbor: Cold Spring Harbor Laboratory Press; 2004.

Ruthazer ES, Li J, Cline HT. Stabilization of axon branch dynamics by synaptic maturation. J Neurosci 2006;26:3594–3603. [PubMed: 16571768]

Sanchez AL, Matthews BJ, Meynard MM, Hu B, Javed S, Cohen Cory S. BDNF increases synapse density in dendrites of developing tectal neurons in vivo. Development 2006;133:2477–2486. [PubMed: 16728478]

Sanes JR, Lichtman JW. Development of the vertebrate neuromuscular junction. Annu Rev Neurosci 1999;22:389–442. [PubMed: 10202544]

Schomberg D, Salzmann M, Stephan D. Enzyme Handbook (Springer). 1993

Shatz CJ, Kirkwood PA. Prenatal development of functional connections in the cat's retinogeniculate pathway. J Neurosci 1984;4:1378–1397. [PubMed: 6726337]

Shepherd GM, Harris KM. Three-dimensional structure and composition of CA3-->CA1 axons in rat hippocampal slices: implications for presynaptic connectivity and compartmentalization. J Neurosci 1998;18:8300–8310. [PubMed: 9763474]

Sin WC, Haas K, Ruthazer ES, Cline HT. Dendrite growth increased by visual activity requires NMDA receptor and Rho GTPases. Nature 2002;419:475–480. [PubMed: 12368855]

Sorensen SA, Rubel EW. The level and integrity of synaptic input regulates dendrite structure. J Neurosci 2006;26:1539–1550. [PubMed: 16452677]

Sretavan D, Shatz CJ. Prenatal development of individual retinogeniculate axons during the period of segregation. Nature 1984;308:845–848. [PubMed: 6201743]

Stepanyants A, Hof PR, Chklovskii DB. Geometry and structural plasticity of synaptic connectivity. Neuron 2002;34:275–288. [PubMed: 11970869]

Toni N, Teng EM, Bushong EA, Aimone JB, Zhao C, Consiglio A, van Praag H, Martone ME, Ellisman MH, Gage FH. Synapse formation on neurons born in the adult hippocampus. Nat Neurosci 2007;10:727–734. [PubMed: 17486101]

Vaughn JE. Fine structure of synaptogenesis in the vertebrate central nervous system. Synapse 1989;3:255–285. [PubMed: 2655146]

Verhage M, Maia AS, Plomp JJ, Brussaard AB, Heeroma JH, Vermeer H, Toonen RF, Hammer RE, van den Berg TK, Missler M, et al. Synaptic assembly of the brain in the absence of neurotransmitter secretion. Science 2000;287:864–869. [PubMed: 10657302]

Wang H, Zhang ZW. A critical window for experience-dependent plasticity at whisker sensory relay synapse in the thalamus. J Neurosci 2008;28:13621–13628. [PubMed: 19074025]

Warton SS, McCart R. Synaptogenesis in the stratum griseum superficiale of the rat superior colliculus. Synapse 1989;3:136–148. [PubMed: 2928962]

Williams CV, McLoon SC. Elimination of the transient ipsilateral retinotectal projection is not solely achieved by cell death in the developing chick. J Neurosci 1991;11:445–453. [PubMed: 1846908]

Wong RO, Ghosh A. Activity-dependent regulation of dendritic growth and patterning. Nat Rev Neurosci 2002;3:803–812. [PubMed: 12360324]

Wu GY, Cline HT. Stabilization of dendritic arbor structure in vivo by CaMKII. Science 1998;279:222–226. [PubMed: 9422694]

Zecevic N, Bourgeois JP, Rakic P. Changes in synaptic density in motor cortex of rhesus monkey during fetal and postnatal life. Brain Res Dev Brain Res 1989;50:11–32.

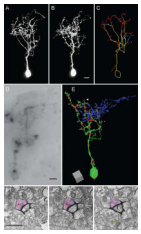

Figure 1. Combined *in vivo* time-lapse imaging and 3D EM reconstruction of a neuron with synaptic inputs

(**A**–**B**) Two-photon images of an optic tectal neuron from a stage 47 tadpole expressing GFP and mHRP collected over a 24h interval. The branch tips marked by 1–4 in **B** are also labeled in **C** and E. (**C**) Drawing of the dendritic arbor of the neuron shown in **A** and **B**. For clarity, the axon is not shown. Branches are color-coded according to their behavior over the previous 24h, yellow: stable; red: extended; blue: retracted. (**D**) Image of a portion of the mHRP-labeled neuron in a vibratome section visualized by the DAB reaction. (**E**) 3D reconstruction of the dendritic arbor of the neuron from 2,381 serial EM micrographs. The dendritic branches and soma are in green and presynaptic terminals are represented by red dots. The white arrowhead marks the dendrite shown in **F**. (**$F_{1–3}$**) Serial EM micrographs of a dendrite from the imaged neuron where the mHRP-labeled plasma membrane is visualized with the nickel-intensified DAB reaction. A synaptic contact site onto the labeled dendrite is marked by the red arrowheads. The axon terminal is colored red. Note that a neighboring presynaptic profile does not form a synapse with the labeled dendrite in these or other serial sections, but does form a synapse with a nearby dendrite, marked by the yellow arrow in F_3. Scale bar is 10μm in **B**, 5μm in **D**, and 500nm in **F**. Scale box in **E** is 5μm.

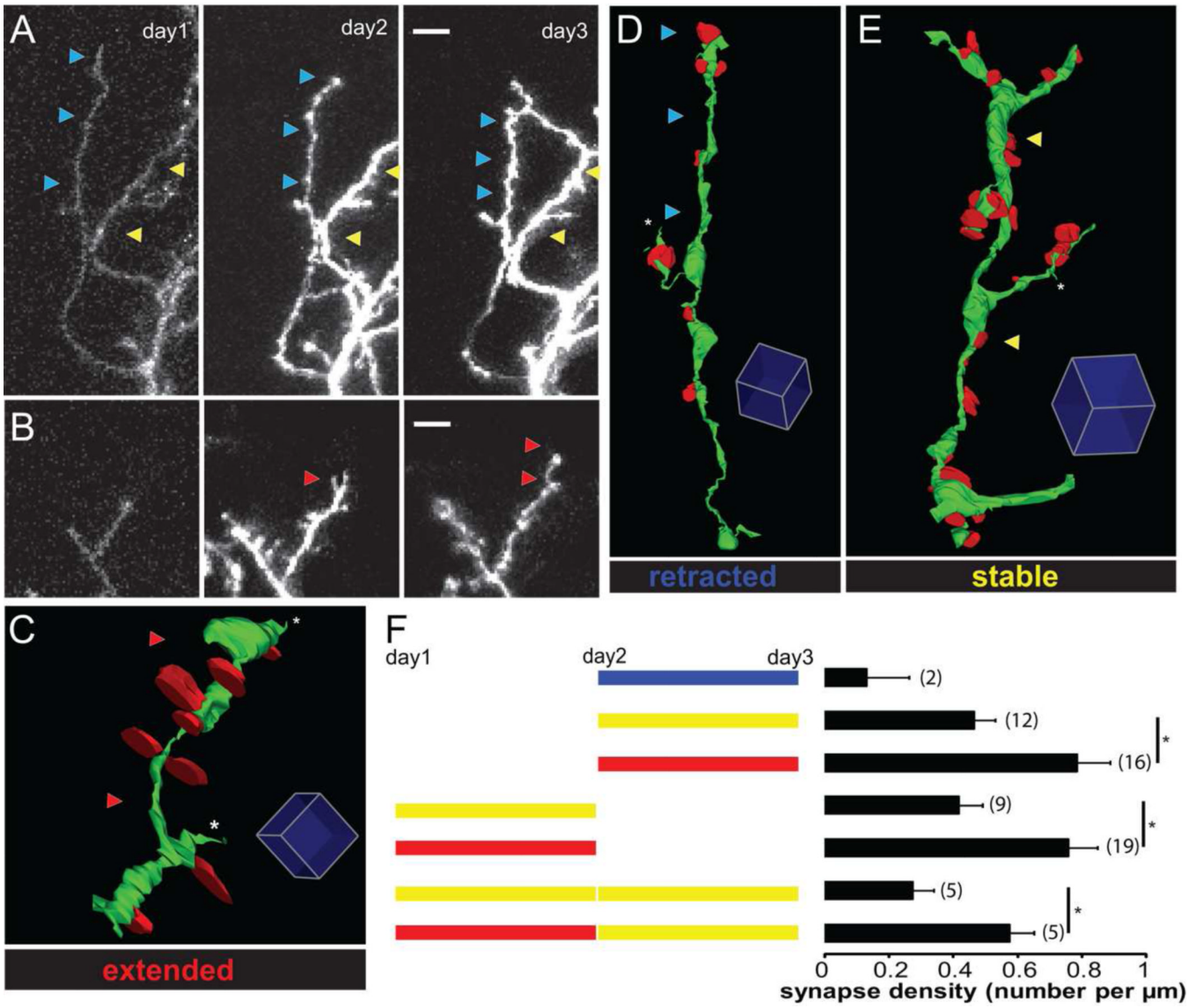

Figure 2. Synapses are eliminated as dendritic branches stabilize

(**A–B**) Two-photon time lapse images showing examples of retracted and stable dendritic branches in **A** and extended branches in **B**. Blue, yellow, and red arrows mark retracted, stable, and extended branches, respectively. (**C–E**) 3D reconstructions from serial EM micrographs of dendritic branches that extended (**C**), retracted (**D**), or were stable (**E**) over the previous 24h. Dendrites are green and their presynaptic inputs are red. Red, blue and yellow arrows mark extended, retracted, and stable branches. (**F**) Diagram of types of branch dynamics that can be visualized with 3 sequential images. Stable branches are shown in yellow, extensions are shown in red and retractions are shown in blue. Dendritic branches were subdivided into different categorizes based on their dynamics over different imaging sessions. The synapse densities of different branch categories are shown in the histograms to the right. Numbers represent the number of branches in each category. Scale bar is 5µm in **A** and **B**. Scale box is 1µm in **C**, 2µm in **D** and **E**.

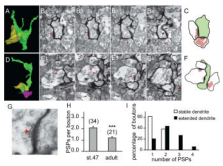

Figure 3. The divergence of contacts from multisynapse boutons decreases as dendrites stabilize

(**A**) 3D reconstruction of a stable branch (green) and one presynaptic axon (yellow). (**$B_{1–4}$**) Serial EM sections through two presynaptic terminals contacting a stable dendritic branch. The synaptic contacts are marked by red arrowheads. (**C**) Diagram of synaptic contacts in B. (**D**) 3D reconstruction of an extended dendritic branch (green) and two presynaptic axons (yellow and pink). (**$E_{1–4}$**) Serial EM sections through two presynaptic terminals contacting an extended dendritic branch and neighboring unlabeled dendrite in **D**. (**F**) Diagram of synaptic contacts in **D**. (**G**) High magnification view of boxed region in E3. (**H**) The number of postsynaptic profiles contacted by each presynaptic bouton decreases significantly from stage 47 tadpole to adult frog. (**I**) The proportion of multisynapse boutons contacting stable and extended dendritic branches according to their number of postsynaptic profiles. Presynaptic boutons contacting stable dendrites (open bars) are less divergent than boutons contacting extending branches (black bars). Scale bar is 500nm in **E** and also applies to **B**.

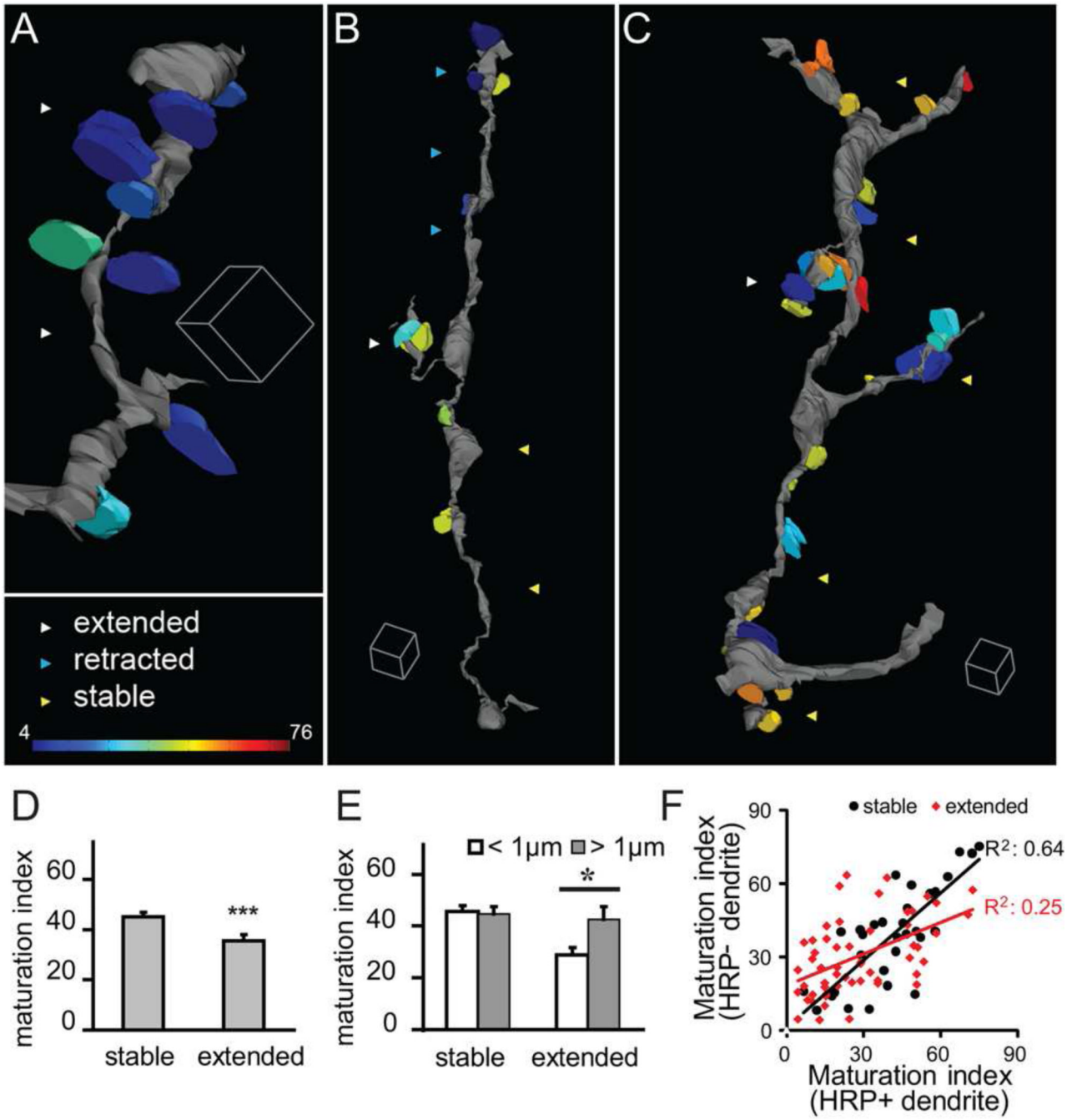

Figure 4. Dynamic branches form clustered immature synapses

(**A–C**) Distribution of synapses, color-coded to show their relative maturation, on 3D renderings of extending (A), retracting (B) and stable (C) dendrites. Immature synapses (cold colors) are preferentially located on dynamic branches; stable branches are studded with mature synapses (warm colors). (**D**) Synapses on stable dendritic branches are more mature than synapses on extended dendritic branches. (**E**) Maturation index of synapses contacting stable and extending branches compared to the distances between synapses (interbouton distance). Extended branches form clustered immature synapses. (**F**) Paired comparison of the maturation indices of synapses from the same axonal bouton contacting mHRP-positive and negative dendrites. Boutons contacting stable HRP-labeled dendrites

also form contacts with relatively correlated maturation indices whereas boutons contacting extending HRP-labeled branches form contacts with heterogeneous maturation indices. Scale box is 1μm in **A**, 2μm in **B** and **C**.

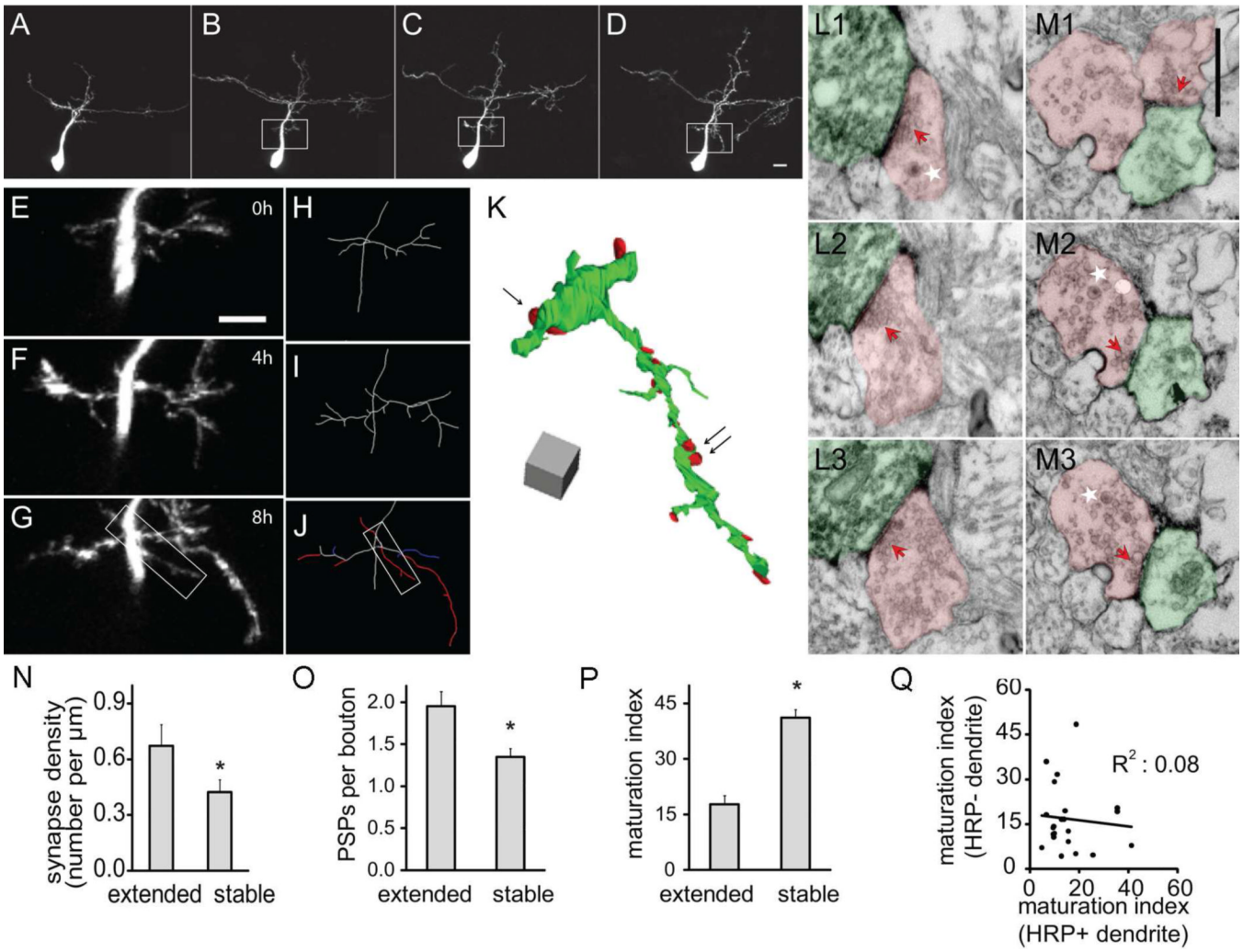

Figure 5. Rapid synapse formation on extended dendritic branches

(**A–D**) Two-photon time-lapse images of an optic tectal neuron from a stage 47 tadpole collected on the second day (**A**) and 0h, 4h, and 8h of the third day (**B–D**) after electroporation. (**E–G**) High magnification view of the region in white boxes of **B–D**. (**H–J**) Drawings of the partial dendritic arbor of the neuron shown in **E–G**. Branches are color-coded according to their dynamics over the previous 4h in **J**. white: stable; red: extended; and blue: retracted. (**K**) 3D reconstruction of the dendritic arbor shown in the white box of **J**. (**L–M**) Serial EM sections through axon terminals contacting branches that were stable (**L1–L3**) or extended (**M1–M3**) over the last 4h. The locations of these two synapses are marked by the single arrow and double black arrows, respectively, in **K**. Axons and dendrites are marked in red and green. Dense core vesicles are marked by white stars and synaptic sites are marked by red arrows. Scale bar in **M1** is 500nm and applies to **L1–M3**. (**N**) Number of postsynaptic partners of axonal boutons contacting stable and extended branches. (**O**) The number of postsynaptic profiles (PSPs) per axonal bouton contacting stable and extended dendritic branches. (**P**) Maturation index of synapses on stable and extended dendritic branches. (**Q**) Paired comparison of maturation index of divergent synapses from the same axonal bouton contacting mHRP-positive and negative dendrites. mHRP positive dendrites extended within past 4 hours.

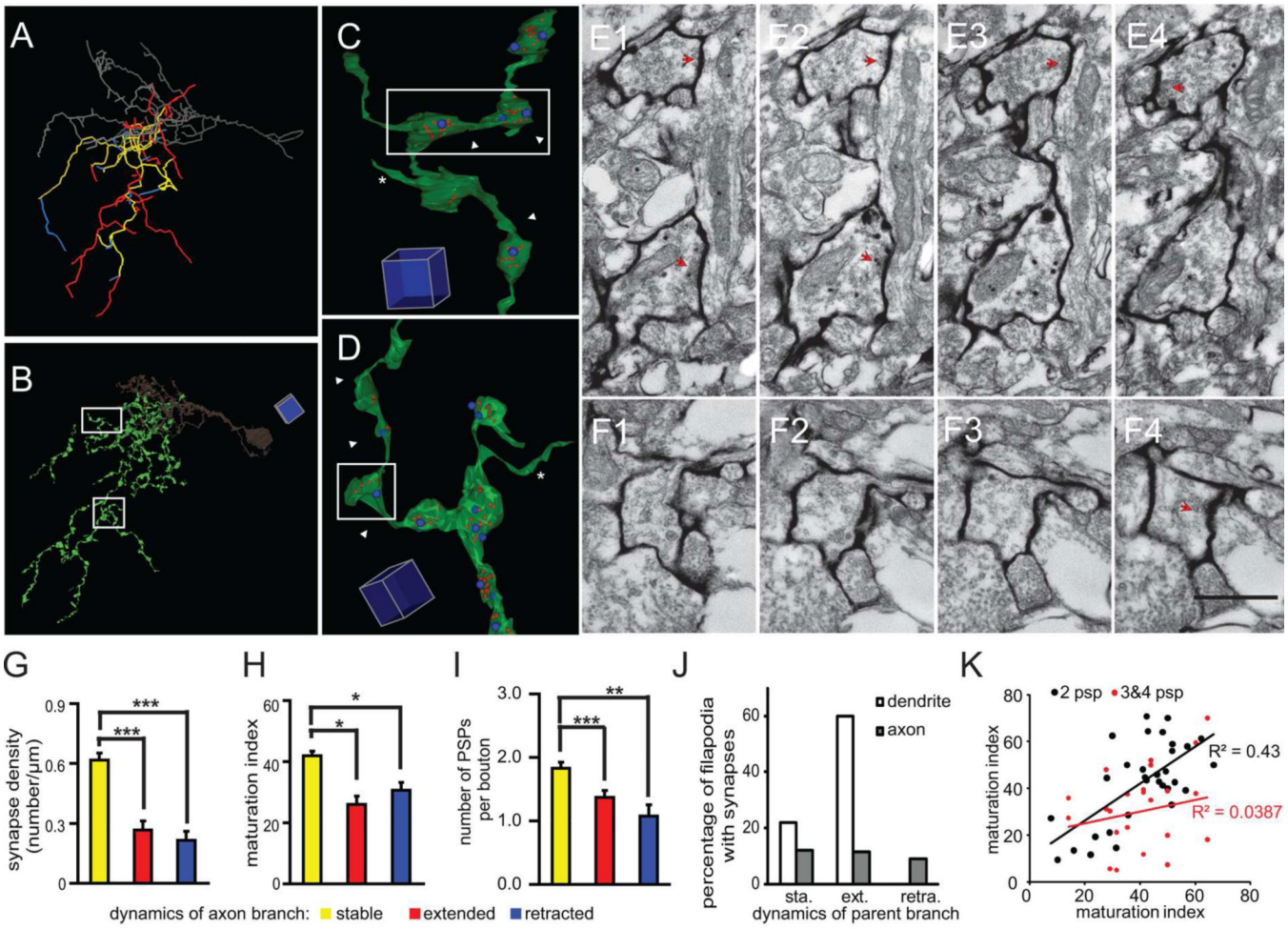

Figure 6. Stable axon branches have a high density of mature synapses

(**A**) Axonal branch drawings with dynamics that are color-coded according to the two-photon time lapse images from day 2–3. Yellow: stable, red: extended, blue: retracted. The dendrite is shown in gray. (**B**) Reconstruction of axonal branches from serial EM sections. (**C**) Example of a stable axonal branch. Blue dots represent postsynaptic profiles, and red dots represent synaptic vesicles labeled by mHRP. (**D**) Example of an extended axon branch marked by white arrowheads. (**E–F**) Serial EM sections show the ultrastructure of axonal boutons from stable and extended branches in $\mathbf{E_{1–4}}$ and $\mathbf{F_{1–4}}$, which are marked by white arrowheads in **C** and **D**, respectively. The synaptic contacts are marked by red arrowheads. (**G**) The density of synaptic contacts from stable, extended, and retracted axon branches. (**H**) Maturation index of axon terminals from stable, extended, and retracted branches. (**I**) Number of connections per bouton from stable, extended, and retracted axon branches. (**J**) Percentage of filopodia emerging from stable, extending or retracting axons and dendrites which form synaptic contacts. About 30% of all axonal filopodia form synapses independent of the dynamic properties of their parent branch. Over 80% of dendritic filopodia form synapses and about 2/3 of them emerge from extending dendrites. (**K**) Maturation indices of synapses from axonal boutons with only 2 PSPs are more correlated than the indices of synapses in boutons contacting 3 or 4 PSPs for multisynapse boutons on extending axon branches. Scale box is 5μm in **B**, 1 μm in **C** and **D**. Scale bar is 500nm in **F** and also applied to **E**. (*: $p<0.05$; **: $p<0.01$; ***: $p<0.001$).

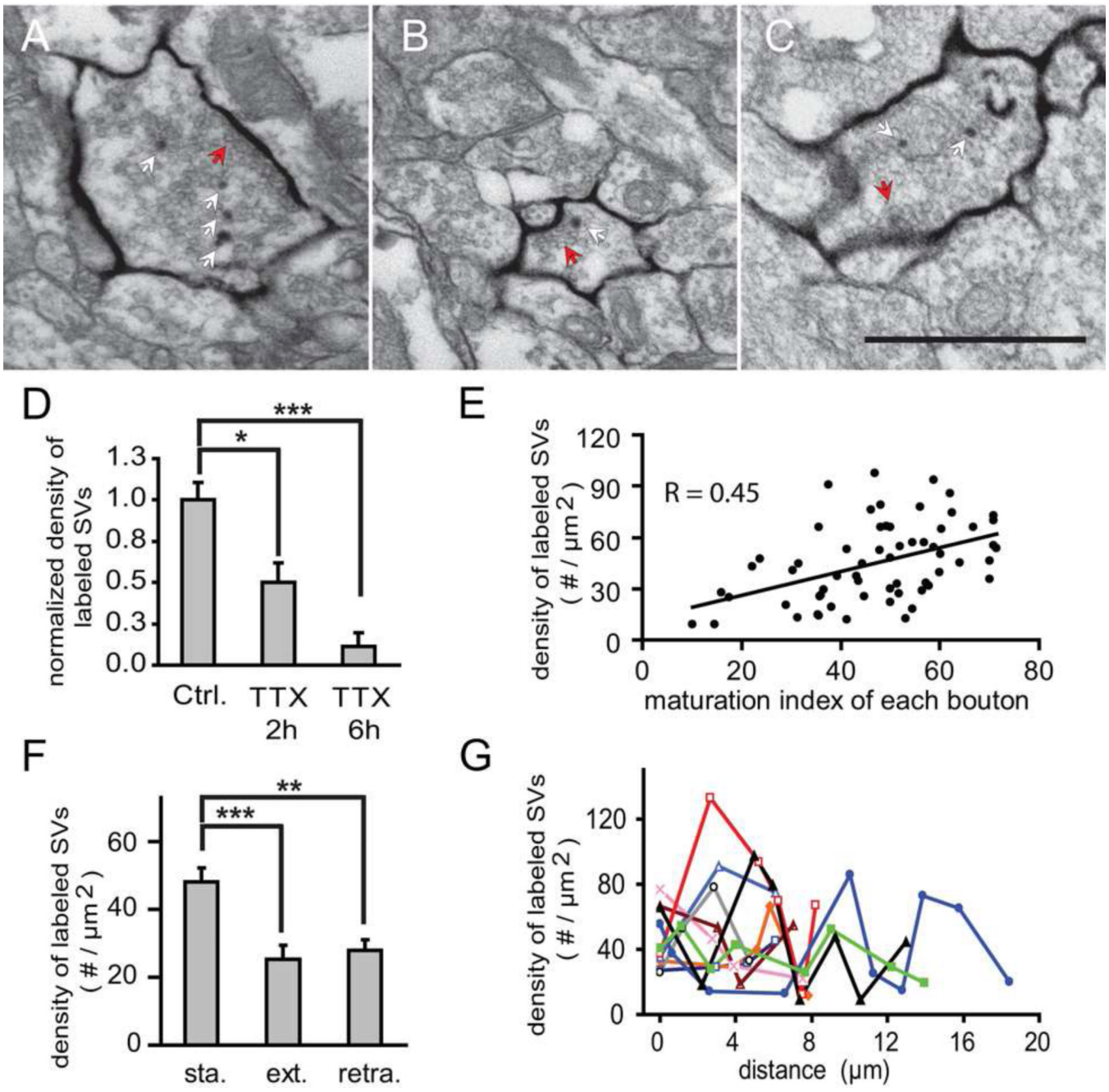

Figure 7. mHRP labels presynaptic vesicles by an activity-dependent mechanism

(**A**) A mature synapse with recycled synaptic vesicles labeled by mHRP. Red arrow points to synaptic contact site and white arrows point to mHRP-labeled presynaptic vesicles. (**B**) An immature synapse with one labeled presynaptic vesicle. (**C**) A mature synapse after incubation in TTX for 2h. (**D**) TTX treatment for 2 and 6h decreases the number of mHRP-labeled synaptic vesicles. (**E**) The density of mHRP-labeled synaptic vesicles correlates with the maturation index of each axonal bouton. (**F**) The density of labeled synaptic vesicles from axon boutons in stable branches is significantly higher than from extended or retracted axonal branches. (**G**) Boutons along an axon have different densities of mHRP-labeled presynaptic vesicles, suggesting that the release behavior of axon boutons is heterogeneous

within the same axon branch. Values for boutons in each axon are connected by colored lines.

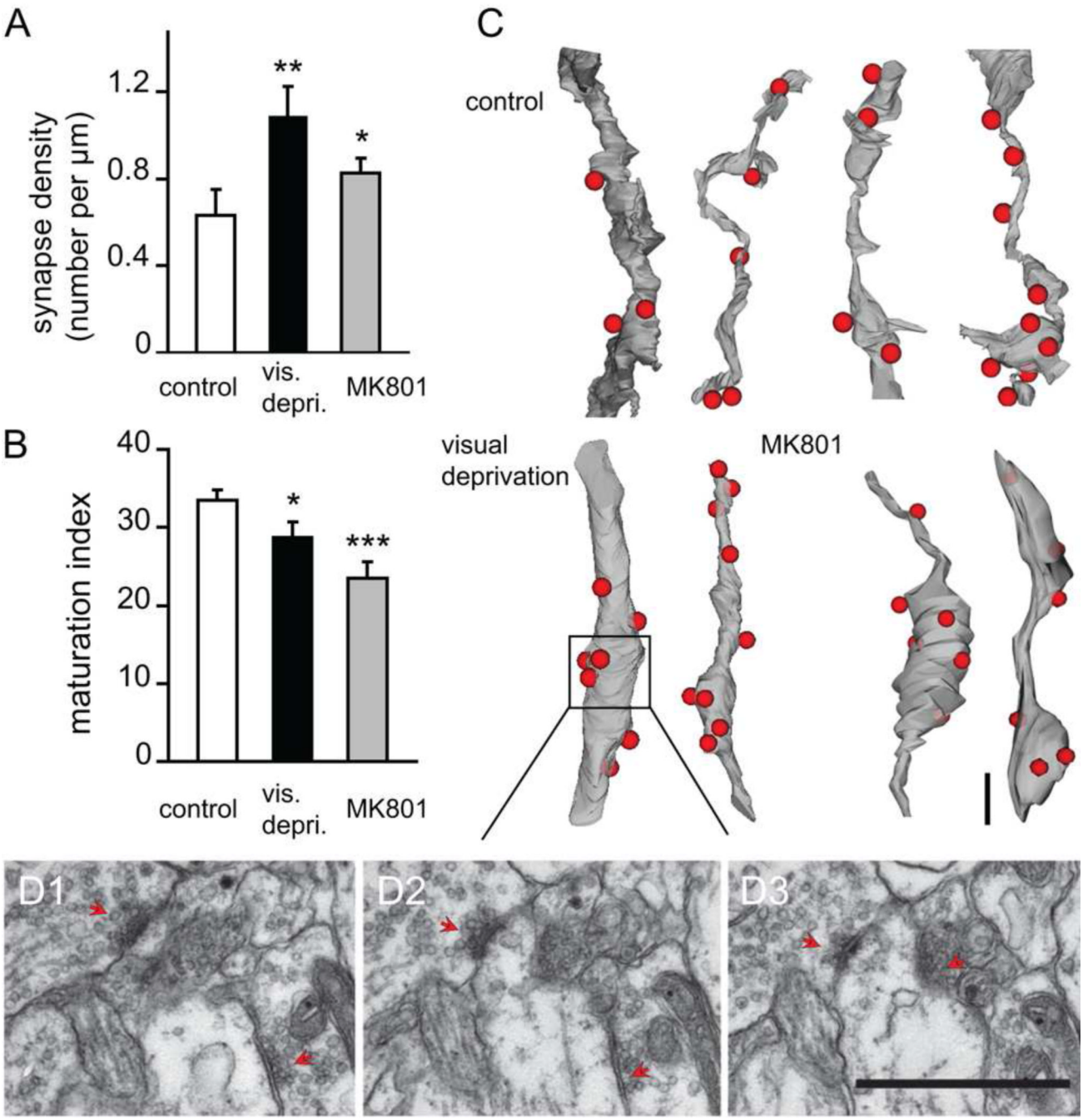

Figure 8. Synapse elimination and synaptic maturation are activity-dependent

(**A**) Synapse density per µm dendritic branch length is significantly greater in visually-deprived (vis. depriv.) and MK801-treated tadpoles. (**B**) Both visual deprivation and MK801 treatment reduce synaptic maturation in the optic tectum. (**C**) 3D reconstructions of dendritic branches under control, visually-deprived, and MK801-treated conditions. Red dots represent synaptic contact sites. (**D1–D3**) Serial electron micrographs show fine morphology of synaptic contacts in **C**. Red arrows point to synapses. Scale bars=1µm.